Optics Letters

Dual-comb coherent Raman spectroscopy with lasers of 1-GHz pulse repetition frequency

Kathrin J. Mohler,[1,2] Bernhard J. Bohn,[1,2] Ming Yan,[1,2] Gwénaëlle Mélen,[2] Theodor W. Hänsch,[1,2] and Nathalie Picqué[1,2,*]

[1]Ludwig-Maximilians-Universität München, Fakultät für Physik, Schellingstrasse 4/III, 80799 München, Germany
[2]Max-Planck-Institut für Quantenoptik, Hans-Kopfermann-Strasse 1, 85748 Garching, Germany
*Corresponding author: nathalie.picque@mpq.mpg.de

We extend the technique of multiplex coherent Raman spectroscopy with two femtosecond mode-locked lasers to oscillators of a pulse repetition frequency of 1 GHz. We demonstrate a spectra of liquids, which span 1100 cm^{-1} of Raman shifts. At a resolution of 6 cm^{-1}, their measurement time may be as short as 5 μs for a refresh rate of 2 kHz. The waiting period between acquisitions is improved 10-fold compared to previous experiments with two lasers of 100-MHz repetition frequencies. © 2017 Optical Society of America

Laser frequency combs enable new approaches to molecular spectroscopy and sensing [1–12]. One of these approaches [7] harnesses coherent nonlinear Raman effects in condensed matter with a pump-probe scheme involving two femtosecond combs of slightly different pulse repetition frequencies. Dual-comb coherent anti-Stokes Raman spectroscopy (CARS) was demonstrated with spectra spanning around 1000 cm^{-1} and measured on a μs-ms time scale with a resolution limited by the intrinsic width of the vibrational molecular bands.

Ref. [7] details the principle of dual-comb coherent Raman spectroscopy. In summary, in the time domain (Fig. 1), the pulses of one comb excite, with a periodicity of $1/(f_{\mathrm{rep}} + \delta f_{\mathrm{rep}})$, low-lying vibrational levels in a Raman two-photon process. The refractive index of the sample is modulated at the vibrational period with a ring-down time related to the coherence time of the transition. After each excitation, the pulse of a second comb of repetition frequency f_{rep} probes the vibrational excitation at a linearly increasing time delay, which is automatically induced by the small difference in repetition frequencies δf_{rep}. The spectrum of the probe comb is alternately blue- and redshifted [13] and its intensity modulation, measured behind an edge spectral filter, directly reveals the frequencies of the excited molecular vibrations with a down-conversion factor equal to $\delta f_{\mathrm{rep}}/f_{\mathrm{rep}}$. A Fourier transform of such time-domain interference computes the Raman spectrum.

As in other dual-comb techniques, the time separation between two pulses of a pump-probe pair is periodically scanned by steps of $\delta f_{\mathrm{rep}}/f_{\mathrm{rep}}^2$ over a range from 0 to $1/f_{\mathrm{rep}}$. Therefore, for an optimal use of the experimental time, the observed decay time of the molecular sample (set by the vibrational coherence time or by the signal-to-noise ratio) should be similar to $1/f_{\mathrm{rep}}$. In the frequency-domain picture, the desired spectral resolution should be comparable to the comb line spacing. The ratio of the comb line spacing to the resolution gives the duty cycle of the acquisition sequence. As the coherence time of the molecular bands in the liquid phase is typically tens of ps, corresponding to line widths of several tens of GHz (several cm^{-1}), frequency combs of large line spacing would benefit from dual-comb CARS. Moreover, the refresh rate δf_{rep} of successive interferograms may be increased as its upper limit scales with the square of the repetition frequency f_{rep}. As detailed in [7], for a spectral span of ΔF (in Hz) in the optical domain, δf_{rep} must indeed be chosen less than or equal to $f_{\mathrm{rep}}^2/(2\Delta F)$ to fulfill the Nyquist
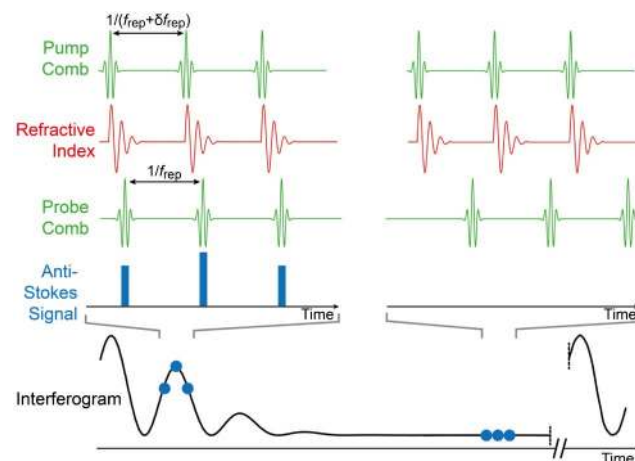

Fig. 1. Time-domain principle of dual-comb CARS. See text and [7] for details.

criterion. However, coherent Raman four-wave mixing signals scale with the cube of the peak power of the laser pulses, making the use of high-repetition-frequency lasers challenging.

The first demonstrations [7] of dual-comb CARS have been performed with 100-MHz oscillators of 20-fs pulse duration and the duty cycle was limited to 3×10^{-3}. In this Letter, we investigate the potential of 1-GHz oscillators for dual-comb CARS.

Figure 2 shows the experimental setup. Two identical titanium-sapphire femtosecond mode-locked lasers (Laser Quantum, Taccor-10s) are used. Their spectrum is centered around 795 nm (12580 cm^{-1}) with a full width at half-maximum (FWHM) of 60 nm (880 cm^{-1}). At the output of the sealed oscillators, the pulses are chirped with a specified group delay dispersion of about $+450 \text{ fs}^2$. Their repetition frequency is around 1 GHz and the difference in repetition frequencies δf_{rep} is chosen between 500 Hz and 2000 Hz. The repetition frequency is controlled by piezo-electric transducers, which adjust the laser cavity length. Low-bandwidth (about 10 kHz) active stabilization is achieved with a servo controller (Laser Quantum, TL-1000), which phase-locks the repetition frequency to an external reference provided by a radio-frequency synthesizer (Rohde & Schwarz, SMA100A-B22). The root-mean-square fluctuations of the repetition frequency are 0.3 Hz over 5 min measured by a 12-digit counter with a gate time of 1s.

The two laser beams are linearly polarized with axes that are not perfectly orthogonal. They are combined on a pellicle beam splitter (Thorlabs, CM1-BP145B2). One output of the beam splitter is used for CARS, as detailed below. The second output measures the residual time-domain interference between the two femtosecond lasers on a fast photodiode (Thorlabs, PDA10A): the sequence of bursts at a period of $1/\delta f_{\text{rep}}$ serves as a trigger signal for the acquisition of the dual-comb coherent Raman interferograms. On the CARS beam path, chirped mirrors (Layertec) compensate for the group delay dispersion (-940 fs^2 in total) in the entire setup (lasers, optical elements before the focal point, air). Spectral shearing interferometry is employed to characterize the ultrashort pulses by means of a SPIDER device (Venteon, Laser Quantum).

A combination of an optical long-wavelength-pass filter (Chroma, ET750lp, optical density: 5, cutoff: 750 nm–13333 cm^{-1}) before the sample, and a short-wavelength-pass filter (Omega Optical, 3RD750SP, transmission <5% for wavelength <750 nm) after the sample separates the anti-Stokes radiation from the light of the titanium-sapphire lasers. The cutoff wavelengths can be slightly changed by tilting the interference filters. The beam is focused with an aspheric lens of a focal length of 8 mm (Newport, 5724) on the liquid sample contained in a 1-mm thick quartz cuvette (Starna, Type 21). At the sample, for each laser the pulse duration is less than
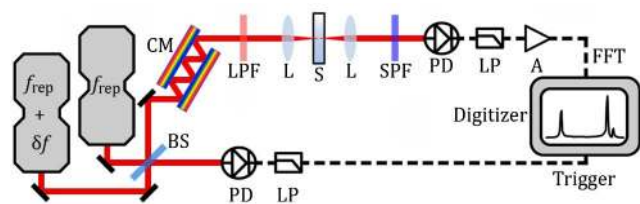
20 fs and the pulse energy is up to 0.5 nJ. The anti-Stokes radiation emerging from the cuvette in the forward direction is collimated by a lens identical to the focusing one. It is optically filtered and focused onto a fast silicon photodiode (Newport, 1621). The interference signal is detected—together with a large background of other signals originating from unfiltered laser radiation—from nonlinear phenomena (including coherent Raman and non-resonant effects) generated at the sample by each laser and from residual intensity noise. The close-to-orthogonal polarizations of the two comb beams diminish the interferometric non-resonant background while retaining a significant part of the resonant contribution to the interference thanks to the depolarization of the sample. Moreover, the non-interferometric signals mostly occur at the repetition frequency of the lasers and their harmonics. Therefore, they can be electrically filtered out. After filtering (Mini Circuits, ZFHP-0R055-S+ and BLP-200+) and amplification (L-3 Narda-MITEQ, AU-1332), the time-domain interference signal is recorded by a data acquisition board (AlazarTech, ATS9360) with a rate of 10^9 samples s^{-1}.

The interferograms are processed by an automated custom MATLAB program. As in other Fourier transform CARS techniques [14–17], the interferometric non-resonant background is present only at short optical delays. It is, therefore, entirely suppressed by suitably positioning the numerical triangular apodization window. The length of the apodization window sets the resolution and the sixfold zero-filling of the interferogram interpolates the spectrum. Only the magnitude spectrum is computed. Phase correction is part of the improvements that need to be implemented in the future. When the two 1-GHz lasers have similar pulse energies at the sample, each laser is alternately the pump and the probe, and the interferograms are symmetric about zero optical delays. For instance, the duty cycle, defined in [7] as the ratio $3.6 f_{\text{rep}}/\delta\nu$, where $\delta\nu$ is the optical resolution, is 2% for an apodized resolution of 6 cm^{-1}. This is 10-fold higher than with 100-MHz systems. Here, however, due to a simplistic trigger of the data acquisition, only one side of the interferogram at about the zero optical delay is recorded and Fourier transformed, thus bringing the actual duty cycle to 1%.

The Fourier transform reveals radio-frequency spectra. Their free spectral range varies from 21 MHz ($\delta f_{\text{rep}} = 500 \text{ Hz}$, down-conversion factor: 5×10^{-7}) to 84 MHz ($\delta f_{\text{rep}} = 2000 \text{ Hz}$, down-conversion factor: 2×10^{-6}). The radio-frequency x-scale is *a posteriori* converted to a scale of optical Raman-shifts by division by the down-conversion factor with the help of the experimentally measured repetition frequencies. The span of Raman shifts converted to wavenumbers is 300–1400 cm^{-1}. It is limited on the low-wavenumber side by the optical filters and on the high-wavenumber side by the spectral bandwidth of the lasers. When spectra are averaged, the wavenumber axis of each individual spectrum is corrected by a multiplying factor prior to averaging. We determine the mean value of the experimental line positions in all the spectra and we multiply the x-scale of each spectrum by a factor that brings the positions to their mean value. This compensates for the residual fluctuations of the difference in repetition frequencies. Such fluctuations induce variations of a couple of kHz of the radio-frequency scale (up to 10 cm^{-1} in the wavenumber scale).

Figure 3 shows two experimental dual-comb CARS spectra of neat toluene measured within times on the microsecond

Fig. 2. Experimental setup for dual-comb CARS using two 1-GHz lasers (see text for details). BS, beamsplitter; CM, chirped mirrors; LPF, long-pass filter; L, lens; S, sample; SPF, short-pass filter; PD, photodetector; LP, electronic long-pass filter; A, amplifier.

scale. No averaging is performed. The apodized resolution is 6 cm^{-1}. Therefore, the spectra comprise 183 spectral elements (defined as span divided by resolution). The duty cycle is 1% if one considers only single-sided interferograms. Five intense lines of toluene centered at 522 cm^{-1}, 788 cm^{-1}, 1001 cm^{-1}, 1028 cm^{-1}, and 1210 cm^{-1}, respectively, are assigned [18] to the ν_{13}, ν_{12}, ν_{11}, ν_{10}, and ν_8 bands, respectively. In Fig. 3(a), the difference in pulse repetition frequencies is $\delta f_{\mathrm{rep}} = 500$ Hz, which leads to a measurement time of 20 μs. The signal-to-noise ratio for the strongest transition at 1001 cm^{-1} is 107. The noise is taken as the standard deviation of the baseline in the wavenumber region around 1350 cm^{-1}. Double-sided interferograms repeat at a refresh time of $1/\delta f_{\mathrm{rep}} = 2$ ms. Every 2 ms it is possible to measure two spectra; each looks like that shown in Fig. 3(a) within 20 μs and with a time separation of a couple of μs set by the apodization window. In Fig. 3(b), as $\delta f_{\mathrm{rep}} = 2000$ Hz, the measurement time is 5 μs, the signal-to-noise ratio is 50, and the refresh time is 500 μs.

When we dilute toluene in 2-propanol, we find that the maxima of the toluene band profiles increase linearly with an increasing concentration. Moreover, we measure (Fig. 4) the dependence of the maximum of the benzene ν_2 band at 992 cm^{-1} with the energy of the pump (resp. probe) pulses. When the energy of the pump (resp. probe) pulses at the sample is varied, the energy of the probe (resp. pump) pulses is kept constant to about 0.4 nJ. We observe that the two curves almost overlap. A fit gives a slope of 1.04 (± 0.02) for the energy dependence of the pump and 1.06 (± 0.03) for that of the probe. The number in parentheses is the statistical uncertainty of the fit. Therefore, the line maxima depend linearly on the concentration of the sample and on the energy of both pump and probe pulses. With coherent Raman signals, a quadratic concentration dependence, as well as an overall cubic energy dependence, is expected. The observed linear behaviors imply that the detected signal results from the interference of the CARS electric field with another field [19,20]. The local oscillator in this additional interference mixing process is the probe beam whose pulses always coincide in time with the interferometric CARS signal at the detector. As the probe beam signal is concentration independent in such configuration, the detector signal is expected to be proportional to the concentration. The interferometric CARS signal scales with the square of pump
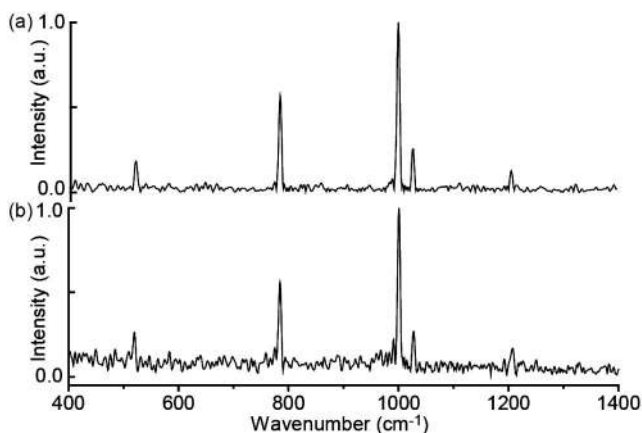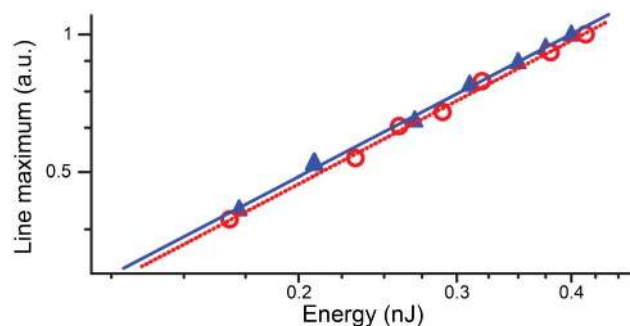

Fig. 4. Dependence of the maximum of the benzene ν_2 line profile at 992 cm^{-1} with the energy of the pump (blue triangles) and probe (open red circles) pulses, on logarithmic x- and y-scales.

pulse energy and with the probe pulse energy. The local oscillator signal scales with the probe pulse energy. Therefore, the detector signal, which results from the interferometric mixing between interferometric CARS and local oscillator signals, has a linear dependence with both the pump and probe pulse energies. In practice, the extent of spectral overlap at the detector between the mutually coherent probe and interferometric CARS signals is experimentally controlled by empirically adjusting the cutoff wavelengths of the optical filters placed before and after the sample. Such heterodyne detection of the weak CARS signal improves the signal-to-noise ratio and provides opportune linear concentration dependence.

Figure 5 presents the spectrum of a mixture of toluene, cyclohexane (band ν_5 at 802 cm^{-1} [21]), and chloroform (band ν_3 at 366 cm^{-1} and band ν_2 at 678 cm^{-1} [22]). The difference in repetition frequencies is $\delta f_{\mathrm{rep}} = 600$ Hz. The apodized resolution is 6 cm^{-1} and 120 spectra are averaged. The measurement time is 2 ms and the total experimental time is 200 ms. Figure 5 illustrates both our broad spectral span—with bands centered at 386 cm^{-1} and at 1210 cm^{-1}—and our resolution, which separates the neighboring transitions of toluene at 788 cm^{-1} and of cyclohexane at 802 cm^{-1}.

Because the CARS signal scales with the cube of the peak power, the main difficulty associated with the use of laser systems of high-repetition frequency is related to the reduced pulse energy at the laser output. We compare the spectrum of toluene of Fig. 3(a) to the same spectrum (Fig. 6) measured with the setup described in [7], where the interferometric CARS signal was not heterodyned with the probe beam. It uses two 100-MHz titanium-sapphire mode-locked lasers, which emit pulses of 20-fs duration. In the spectrum of Fig. 6, the pulse energy at
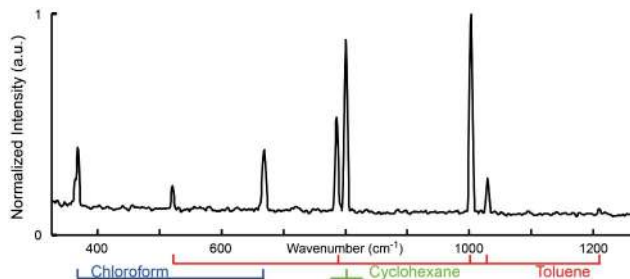

Fig. 3. Experimental spectra of toluene measured at 6 cm^{-1} resolution within (a) 20 μs and (b) 5 μs.

Fig. 5. Dual-comb CARS spectrum of toluene, chloroform and cyclohexane with a mixing ratio of 1:1:1.
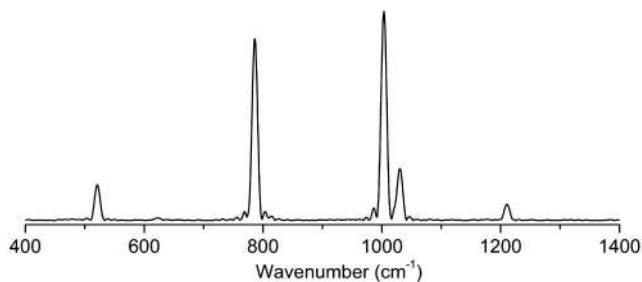
Fig. 6. Experimental dual-comb spectrum of toluene, measured with two 100-MHz femtosecond lasers.

the sample is 4 nJ per laser, the difference in repetition frequencies is 50 Hz, and the apodized resolution is 6 cm^{-1}. The recording time is 20 μs, which is identical to the spectrum shown in Fig. 3(a). The signal-to-noise ratio of the most intense toluene band at 1001 cm^{-1} is 1020. Therefore, for the same measurement time, the spectrum recorded with the 1-GHz dual-comb system [Fig. 3(a)] has a signal-to-noise ratio of about one order of magnitude worse than the spectrum measured with the 100-MHz system whereas the pulse energy is eightfold weaker—therefore, the CARS signal is 512 times fainter. Such favorable scaling may be explained by several factors. The number of pump-probe sequences during the measurement time is 10 times higher with the 1-GHz system than with that of 100 MHz. The heterodyne detection—by mixing with the local oscillator field of the spectrally overlapping probe laser beam—benefits the signal-to-noise ratio.

Such results contribute to a current effort to increase the acquisition speeds and rates of techniques of broadband nonlinear Raman spectroscopy (e.g., [23–28]). Moreover, direct frequency comb spectroscopy of samples in the condensed phase attracts growing interest [7–12]. Such experiments will benefit [29] from frequency combs of large line spacing and might trigger the development of dedicated laser sources. While linear-absorption dual-comb spectroscopy [9–11] may straightforwardly take advantage of such combs of high-repetition frequency, nonlinear dual-comb spectroscopy of transitions of short coherence times still calls for optimized strategies. In this Letter, we demonstrate that mode-locked lasers of 1-GHz repetition frequency can be successfully harnessed for coherent Raman dual-comb spectroscopy of neat liquids. We experimentally show duty cycles that are 10-fold better than with lasers of a repetition frequency of 100 MHz [7], as well as refresh times that are improved 20-fold. The span of the 1-GHz lasers of 1500 cm^{-1} allows, in principle, refresh rates δf_{rep} up to about 10 kHz but improvements to the signal-to-noise ratio will then be required. With such future enhancements to the signal-to-noise ratio and with the recent availability of commercial Ti:Sa femtosecond oscillators of 10-GHz repetition frequency, the full potential of dual-comb coherent Raman spectroscopy without moving parts may be realized [30]. Broadband dual-comb Raman spectra measured on a microsecond-scale at a refresh rate of several tens of kHz may become within reach and dual-comb CARS might evolve into a powerful tool for studies of short-lived transient species, high-sensitivity experiments requiring efficient signal averaging, or fast hyper-spectral imaging.

REFERENCES

1. M. J. Thorpe, K. D. Moll, R. J. Jones, B. Safdi, and J. Ye, Science **311**, 1595 (2006).
2. S. A. Diddams, L. Hollberg, and V. Mbele, Nature **445**, 627 (2007).
3. I. Coddington, W. C. Swann, and N. R. Newbury, Phys. Rev. Lett. **100**, 013902 (2008).
4. J. Mandon, G. Guelachvili, and N. Picqué, Nat. Photonics **3**, 99 (2009).
5. B. Bernhardt, A. Ozawa, P. Jacquet, M. Jacquey, Y. Kobayashi, T. Udem, R. Holzwarth, G. Guelachvili, T. W. Hänsch, and N. Picqué, Nat. Photonics **4**, 55 (2010).
6. A. Hipke, S. A. Meek, T. Ideguchi, T. W. Hänsch, and N. Picqué, Phys. Rev. A **90**, 011805(R) (2014).
7. T. Ideguchi, S. Holzner, B. Bernhardt, G. Guelachvili, N. Picqué, and T. W. Hänsch, Nature **502**, 355 (2013).
8. T. Ideguchi, B. Bernhardt, G. Guelachvili, T. W. Hänsch, and N. Picqué, Opt. Lett. **37**, 4498 (2012).
9. T. Ganz, M. Brehm, H. G. von Ribbeck, D. W. van der Weide, and F. Keilmann, New J. Phys. **10**, 123007 (2008).
10. A. Asahara, A. Nishiyama, S. Yoshida, K. Kondo, Y. Nakajima, and K. Minoshima, Opt. Lett. **41**, 4971 (2016).
11. A. Ishizawa, T. Nishikawa, M. Yan, G. Millot, H. Gotoh, T. W. Hänsch, and N. Picqué, *CLEO: 2015*, OSA Technical Digest (online) (Optical Society of America, 2015), paper SW1G.7.
12. S. Avino, A. Giorgini, M. Salza, M. Fabian, G. Gagliardi, and P. De Natale, Appl. Phys. Lett. **102**, 201116 (2013).
13. Y. Yan, E. B. Gamble, and K. A. Nelson, J. Chem. Phys. **83**, 5391 (1985).
14. N. Dudovich, D. Oron, and Y. Silberberg, J. Chem. Phys. **118**, 9208 (2003).
15. J. P. Ogilvie, E. Beaurepaire, A. Alexandrou, and M. Joffre, Opt. Lett. **31**, 480 (2006).
16. B. von Vacano and M. Motzkus, Phys. Chem. Chem. Phys. **10**, 681 (2008).
17. K. Isobe, A. Suda, M. Tanaka, H. Hashimoto, F. Kannari, H. Kawano, H. Mizuno, A. Miyawaki, and K. Midorikawa, Opt. Express **17**, 11259 (2009).
18. T. H. S. Bican, H. W. Schrotter, and V. Mohacek Grosev, J. Raman Spectrosc. **26**, 787 (1995).
19. M. Cui, J. Skodack, and J. P. Ogilvie, Appl. Opt. **47**, 5790 (2008).
20. E. O. Potma, C. L. Evans, and X. S. Xie, Opt. Lett. **31**, 241 (2006).
21. K. B. Wiberg and A. Shrake, Spectrochim. Acta A **27**, 1139 (1971).
22. K. Kim and W. T. King, J. Chem. Phys. **80**, 978 (1984).
23. C. H. Camp, Jr. and M. T. Cicerone, Nat. Photonics **9**, 295 (2015).
24. S. R. Domingue, D. G. Winters, and R. A. Bartels, Opt. Lett. **39**, 4124 (2014).
25. M. Tamamitsu, Y. Sakaki, T. Nakamura, G. K. Podagatlapalli, T. Ideguchi, and K. Goda, Vib. Spectrosc. in press (2016).
26. L. Czerwinski, J. Nixdorf, G. Di Florio, and P. Gilch, Opt. Lett. **41**, 3021 (2016).
27. F. Saltarelli, V. Kumar, D. Viola, F. Crisafi, F. Preda, G. Cerullo, and D. Polli, Opt. Express **24**, 21264 (2016).
28. J. Réhault, F. Crisafi, V. Kumar, G. Ciardi, M. Marangoni, G. Cerullo, and D. Polli, Opt. Express **23**, 25235 (2015).
29. M. Yu, Y. Okawachi, A. G. Griffith, N. Picqué, M. Lipson, and A. L. Gaeta, "Silicon-chip-based mid-infrared dual-comb spectroscopy," preprint at arXiv:1610.01121 (2016).
30. G. Mélen, M. Yan, P.-L. Luo, T. W. Hänsch, and N. Picqué, *Light, Energy and the Environment Congress*, OSA Technical Digest (online) (Optical Society of America, 2016), paper FW2E.3.